INFLUENCE OF SOLIDIFICATION SPEED ON THE STRUCTURE AND MAGNETIC PROPERTIES OF $Nd_{10}Fe_{81}Zr_1B_6$ IN THE AS-CAST STATE

VPLIV HITROSTI STRJEVANJA NA STRUKTURO IN MAGNETNE LASTNOSTI ZLITINE $Nd_{10}Fe_{81}Zr_1B_6$ V LITEM STANJU

Marcin Dośpiał, Marcin Nabiałek

Czestochowa University of Technology, Institute of Physics, Armii Krajowej Av. 19, 42-200 Czestochowa, Poland
mdospial@wp.pl

The paper presents results of the structure and magnetic properties of the $Nd_{10-x}Tb_xFe_{81}Zr_1B_6$ ($x = 0$, 2) alloy in the as-cast state. The samples were produced using the melt-spinning method. The solidification speed was controlled indirectly by changing the linear velocity of a copper drum. Based on magnetic and structural studies, it was found that samples obtained while the linear velocity of the copper drum was equal to 20 m/s had good hard-magnetic properties. The substitution of 2 % of Nd by Tb led to grain growth of both the α-Fe (9 nm and 24 nm for $x = 0$ and $x = 2$) and $Nd_2Fe_{14}B$ phases (41 nm and 70 nm for $x = 0$ and $x = 2$, respectively). The grain growth to sizes higher than the exchange interaction distance in the sample with Tb resulted in a bimodal shape of the demagnetization curve. The samples obtained at higher linear speeds of the copper drum were composed of amorphous matrices with small amounts of crystalline phases and had weak, soft-magnetic properties.

Keywords: permanent magnets, nanocomposites, X-ray diffraction, exchange interactions

Članek predstavlja rezultate študije strukturnih in magnetnih lastnosti zlitine $Nd_{10-x}Tb_xFe_{81}Zr_1B_6$ ($x = 0$, 2) v litem stanju. Vzorci so bili pripravljeni z ulivanjem na hitro vrtečem se valju. Hitrost strjevanja je bila posredno kontrolirana s spreminjanjem linearne hitrosti bakrenega valja. Magnetne in strukturne študije so pokazale, da imajo vzorci, dobljeni pri linearni hitrosti bakrenega valja 20 m/s, dobre trdomagnetne lastnosti. Nadomestilo z 2 % atomskega deleža Nd s Tb, je povzročilo rast zrn obeh faz α-Fe (9 nm in 24 nm pri $x = 0$ in $x = 2$) in $Nd_2Fe_{14}B$ (41 nm in 70 nm pri $x = 0$ in $x = 2$). Rast zrn, do velikosti, večje od izmenjalne interakcijske razdalje v vzorcu s Tb, se je pokazala v bimodalni obliki demagnetizacijske krivulje. Vzorci, dobljeni pri večjih linearnih hitrostih bakrenega valja, so bili sestavljeni iz amorfne osnove z majhnim deležem kristalnih faz in so imeli slabe mehko magnetne lastnosti.

Ključne besede: permanentni magneti, nanokompoziti, rentgenska difrakcija, izmenjalne interakcije

1 INTRODUCTION

Alloys based on rare earths, iron and boron are currently some of the most popular groups of materials with hard magnetic properties. These materials are widely used in the electro-engineering industry. In recent years, many scientific and industrial units have been carrying out research on methods for curing their magnetic properties.[1–5] The studies were mainly focused on slight modifications to the chemical composition and modifications to the production process parameters.

The most effective process, which guarantees repeatability of the functional properties of produced alloys, is producing amorphous ribbons and then tailoring their properties by an appropriately matched heat treatment.[6] However, the application of the heat treatment generates additional costs. An alternative approach is solidification of the liquid alloy with a slow speed. This leads to a material with hard magnetic properties in the as-cast state. A drawback of this method is the poor repeatability of the functional parameters.

Modifications to the composition by a partial substitution of Nd by Tb can lead to two outcomes: if an excess amount of Tb is used, it can result in the formation of an amorphous matrix dividing the $Nd_2Fe_{14}B$ grains, thereby leading to a higher coercivity and also a significantly reduced remanence;[7,8] if smaller amounts of rare earths with respect to the stoichiometric $Nd_2Fe_{14}B$ composition are used, it may result in the formation of nanocomposites consisting of both $Nd_2Fe_{14}B$ and α-Fe grains. The proper selection of the production process parameters leads to grains of soft magnetic phase with sizes similar or smaller than the exchange-interaction length. This allows obtaining hard magnetic materials with high saturation magnetization and a significant remanence.[8,9]

Motivated by the above idea, we studied the influence of cooling rate on the curing of magnetic properties and the structure of $Nd_{10-x}Tb_xFe_{81}Zr_1B_6$ ($x = 0$ and $x = 2$) alloys, in the as-cast state, and the results of the study we report in this paper.

2 EXPERIMENTAL DETAILS

The research material, i.e., $Nd_{10-x}Tb_xFe_{81}Zr_1B_6$ ($x = 0$, 2) melt, was obtained from components of the following
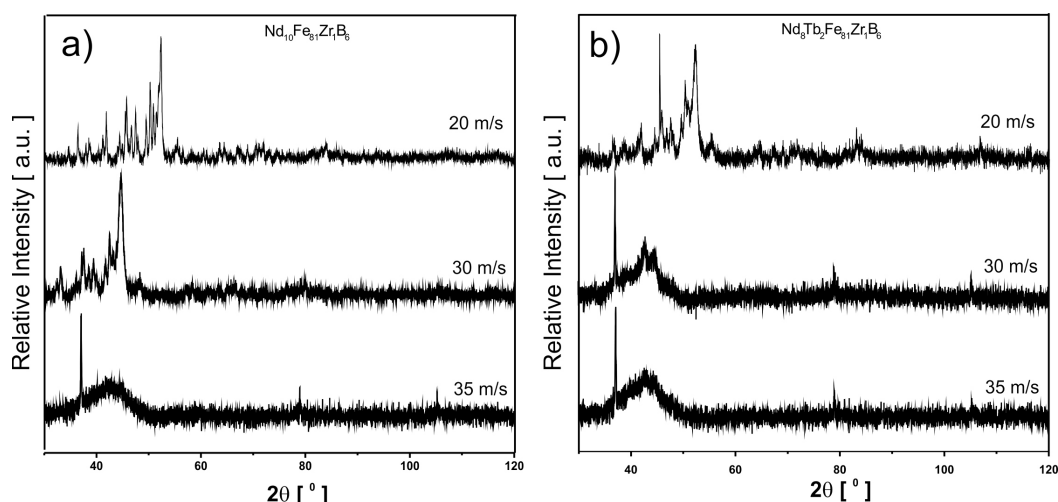
Figure 1: X-ray diffraction patterns of: a) $Nd_{10}Fe_{81}Zr_1B_6$, b) $Nd_8Tb_2Fe_{81}Zr_1B_6$ alloys obtained at different cooling rates, for samples in the as-cast state
Slika 1: Rentgenska difrakcija: a) $Nd_{10}Fe_{81}Zr_1B_6$, b) $Nd_8Tb_2Fe_{81}Zr_1B_6$ zlitin, dobljenih pri različnih hitrostih ohlajanja, za vzorce v litem stanju

purity: Fe – 99.99 %; Zr – 99.99 %; Nd – 99.95 %, Tb – 99.95 %, B – 99.99 %. The crystalline ingots were several times remelted to ensure the best mixing of elements constituting the investigated material. Thin tapes were produced by a unidirectional solidification of liquid metal on a rotating copper cylinder, with three different linear velocities (20, 30 and 35) m/s. The microstructure of the samples, in the as-cast state, was examined using a Bruker D8 Advance X-ray diffractometer with a characteristic Cu-K_α radiation source (0.154056 nm). The samples were scanned in the 2θ angle range from 30° to 120° with a resolution of 0.02° and an exposure time of 3 s per step. Two samples were chosen for further analyses, both qualitative and quantitative. Phase-composition

analysis was performed using the Rietveld method. The magnetic studies were performed using a LakeShore vibrating-sample magnetometer in an external magnetic field up to 2 T. The demagnetization coefficient dependent on the shape of the sample was not taken into account. All the measurements were performed at room temperature.

3 RESULTS AND DISCUSSION

Figure 1 shows the X-ray diffraction patterns obtained for $Nd_{10-x}Tb_xFe_{81}Zr_1B_6$ ($x = 0$, 2) samples in the form of tapes, in the as-cast state.

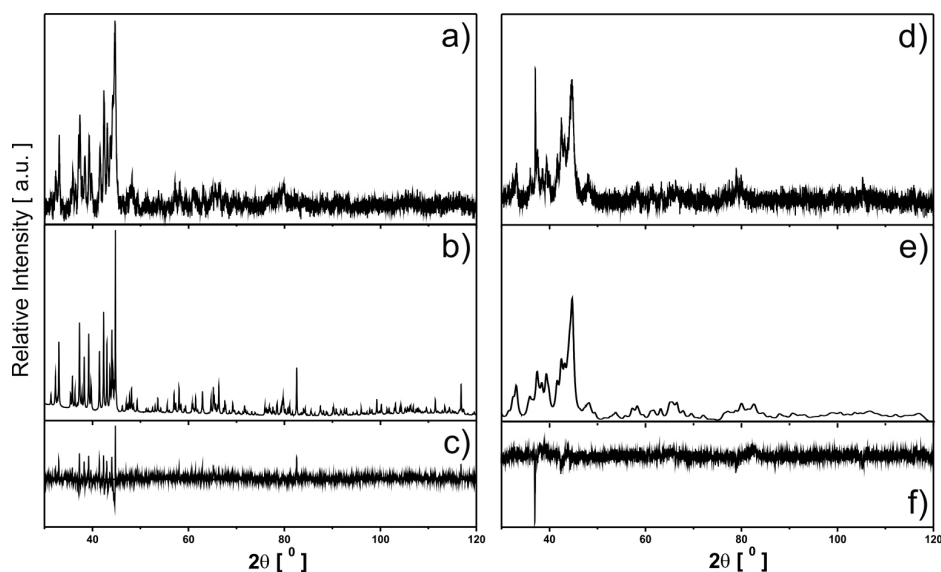**Figure 2:** Quantitative match of the phase composition obtained using the Rietveld refinement method for: a), c) $Nd_{10}Fe_{81}Zr_1B_6$, d), f) $Nd_8Tb_2Fe_{81}Zr_1B_6$ alloys solidified at 20 m/s linear velocity of copper drum, where a), d) experimental curve, b), e) matched pattern and c), f) difference plot
Slika 2: Kvantitativno ujemanje sestave faz, dobljene z Rietveldovo metodo izpopolnitve: a), c) $Nd_{10}Fe_{81}Zr_1B_6$, d), f) $Nd_8Tb_2Fe_{81}Zr_1B_6$ zlitini strjeni pri linearni hitrosti bakrenega valja 20 m/s, kjer sta a), d) eksperimentalni krivulji, b), e) ujemanje in c), f) diagram razlik

In all the diffraction patterns obtained for the samples cooled at higher rates, corresponding to the drum linear speeds of 30 m/s and 35 m/s, at a 2θ angle of about 43° a broad, diffused halo characteristic for materials containing an iron-based amorphous phase is present. Also, it is possible to distinguish the presence of narrower peaks originating from small inclusions of crystalline phases. Similar patterns were described in the literature as semi-crystalline structures.[10,11]

The diffraction patterns of the samples solidified at a drum speed of 20 m/s were composed of a number of narrow peaks characteristic for a crystalline structure. In this case, no diffused halo was observed, which indicates the absence of any amorphous phase. A comparison of the experimental diffraction peaks with the EVA database let us conclude that two crystalline phases were present in the sample: α-Fe and $Nd_2Fe_{14}B$. These results are in agreement with other reports concerned on $Nd_2Fe_{14}B$ alloys with an over-stoichiometric iron content.[7,12–13]

To ascertain quantitatively the phase compositions of the samples without an amorphous matrix, Rietveld analysis was performed (**Figure 2**), and the matching results are summarized in **Tables 1** and **2**.

Table 1: The qualitative phase composition of $Nd_{10-x}Tb_xFe_{81}Zr_1B_6$ (where $x = 0$ or 2) samples solidified with the linear velocity of the copper drum of 20 m/s, determined using the Rietveld refinement method
Tabela 1: Kvalitativna sestava faz $Nd_{10-x}Tb_xFe_{81}Zr_1B_6$, (kjer je $x = 0$ ali 2), strjenih vzorcev z linearno hitrostjo bakrenega valja 20 m/s, določena z uporabo Rietveldove metode izpopolnitve

Phase composition		
Alloy	α-Fe (% vol)	$RE_2Fe_{14}B$ (% vol)
$Nd_{10}Fe_{81}Zr_1B_6$	19.15	80.85
$Nd_8Tb_2Fe_{81}Zr_1B_6$	19.40	80.60

Table 2: Matching coefficients of the quantitative phase composition of $Nd_{10-x}Tb_xFe_{81}Zr_1B_6$ (where $x = 0$ or 2) samples solidified with the linear velocity of the copper drum of 20 m/s, determined using the Rietveld refinement method
Tabela 2: Koeficienti ujemanja kvantitativne sestave faze $Nd_{10-x}Tb_xFe_{81}Zr_1B_6$ (kjer je $x = 0$ ali 2) strjenih vzorcev z linearno hitrostjo bakrenega valja 20 m/s, določeno z uporabo Rietveldove metode izpopolnitve

R – match parameters			
Alloy	R_p	R_{wp}	R_{exp}
$Nd_{10}Fe_{81}Zr_1B_6$	46.11	197.03	0.18
$Nd_8Tb_2Fe_{81}Zr_1B_6$	44.15	192.79	0.11

The average grain size was determined on the basis of Bragg's equation for the 10 and 3 most intense peaks of the $Nd_2Fe_{14}B$ and α-Fe, respectively:[14]

$$\Delta^{hkl}(2\theta) \cdot \cos(\theta_B^{hkl}) = \frac{K \cdot \lambda}{D} + 2\frac{\Delta d}{d} \cdot \sin(\theta_B^{hkl}) \qquad (1)$$

where D is the average grain size, K is a shape factor of 0.89, λ is the X-ray wavelength, and Δ^{hkl} is the half-width of the peak, $\Delta d/d$ is the relative deformation of the crystalline lattice and θ_B^{hkl} is the Bragg angle.

The above-presented equation describes the effect of the grain size and the relative deformation of the crystalline lattice resulting from diffraction-peak broadening. This relationship is linear and the grain size is determined from the intersection of the ordinate axis.

The average grain size of the α-Fe and $Nd_2Fe_{14}B$ phases was 9 nm and 41 nm, respectively, for $Nd_{10}Fe_{81}Zr_1B_6$, and 24 nm and 70 nm for the alloy $Nd_8Tb_2Fe_{81}Zr_1B_6$ for samples solidified at a drum linear velocity of 20 m/s. Due to the low intensity of the peaks originating from the crystalline phases, for samples solidified at higher linear velocities of the copper drum, the particle size was not determined.
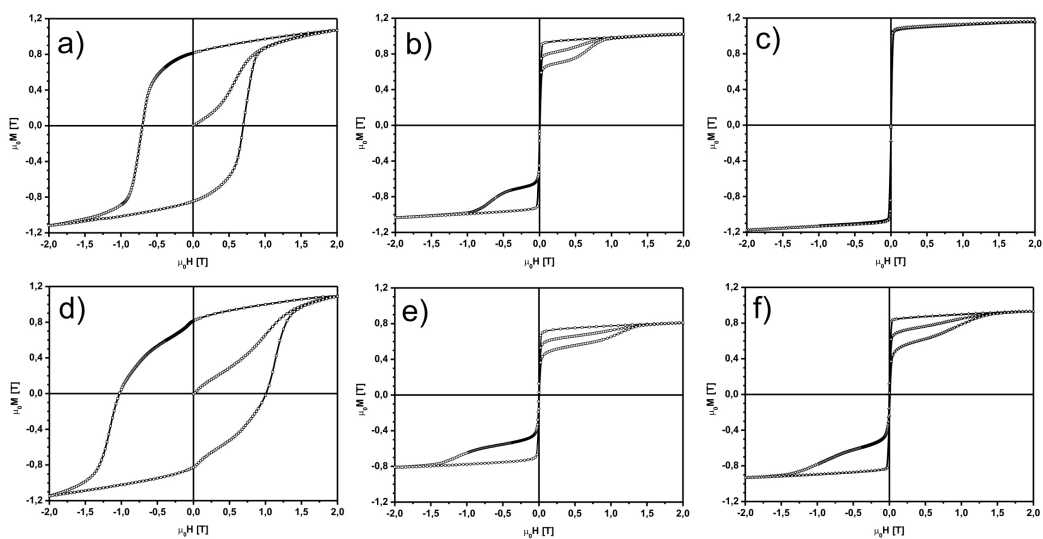
Figure 3: The magnetic hysteresis loops and the initial magnetization curves for the: a), c) $Nd_{10}Fe_{81}Zr_1B_6$ and d), f) $Nd_8Tb_2Fe_{81}Zr_1B_6$ alloys, solidified at linear speeds of the copper drum equal to: a), d) 20 m/s, b), e) 30 m/s, c), f) 35 m/s
Slika 3: Magnetne histerezne zanke in začetne krivulje magnetizacije pri zlitinah: a), c) $Nd_{10}Fe_{81}Zr_1B_6$ in d), f) $Nd_8Tb_2Fe_{81}Zr_1B_6$, strjenih pri linearni hitrosti bakrenega valja: a), d) 20 m/s, b), e) 30 m/s, c), f) 35 m/s

Figure 3 shows the magnetic hysteresis loops and the initial magnetization curves for all the studied samples.

From the analysis of the initial magnetization curves and the main hysteresis loops the magnetic parameters, such as coercivity ($_JH_C$), remanence ($\mu_0 M_R$) and saturation of the magnetization ($\mu_0 M_S$), were determined (**Table 3**). Additionally, for the materials with the best hard magnetic properties the ratio M_R/M_S was also calculated. It allows estimating the extent to which, in the nanocomposite, the phases with hard and soft magnetic properties are coupled by means of exchange interactions.[12,15,16] An additional indicator proving information about the existence of such interactions in the nanocomposite comprising the phases of different magnetic hardness can be the shape of the magnetic hysteresis loop in combination with the results of the phase composition and grain size studies.[15–17]

Table 3: The basic magnetic parameters of the studied $Nd_{10-x}Tb_xFe_{81}Zr_1B_6$ (where $x =0$ or 2) tapes in the as-cast state, determined from the initial magnetization curves and magnetic hysteresis loops
Tabela 3: Osnovne magnetne lastnosti proučevanih $Nd_{10-x}Tb_xFe_{81}Zr_1B_6$ (kjer je $x = 0$ ali 2) trakov v litem stanju, določenih iz začetnih magnetizacijskih krivulj in magnetnih histereznih zank

Linear velocity v (m/s)	coercivity $_JH_C$ (T)	remanence $\mu_0 M_R$ (T)	M_R/M_S ratio (a.u.)	Saturation of the magnetization $\mu_0 M_S$ (T)
$Nd_{10}Fe_{81}Zr_1B_6$				
20	0,7	0,82	0,77	1,06
30	9×10^{-4}	–	–	1,02
35	4×10^{-4}	–	–	1,15
$Nd_8Tb_2Fe_{81}Zr_1B_6$				
20	1,03	0,81	0,73	1,10
30	54×10^{-4}	–	–	0,81
35	13×10^{-4}	–	–	0,93

Based on the data collected in **Table 3**, it was found that the material solidified at higher linear speeds of the rotating copper drum (30 m/s and 35 m/s) was characterized by poor, soft-magnetic properties, which was related to the polycrystalline structure. Inclusions of nanocrystalline grains in the amorphous matrix led to the formation of additional pinning sites, which increases the coercivity of the sample. Tapes produced with the lowest cooling rates (20 m/s drum speed) were characterized by good hard magnetic properties. The substitution of Nd by Tb in the $Nd_{10-x}Tb_xFe_{81}Zr_1B_6$ alloy, quenched with the lowest cooling rate resulted in an improvement of the saturation magnetization and in a significant increase in the coercivity. The increase in the saturation magnetization was associated with a slightly higher content of α-Fe phase in the alloy composition.

The shape of the magnetic hysteresis loop of a $Nd_{10}Fe_{81}Zr_1B_6$ sample with hard magnetic properties was smooth, in spite of the presence of the two phases with different magnetic hardnesses. Additionally, a high M_R/M_S ratio (greater than 0.5) and a moderate grain size

of both phases are evidence of a strong coupling between the grains of different phases, through exchange interactions. The change of 2 % in the fractions of Nd by Tb in the atomic composition, while maintaining the same cooling rate, caused the formation of a bimodal shape of the hysteresis loop. Juxtaposing this with the much larger average grain size of both phases (almost two times higher) and a lower M_R/M_S ratio, it can be concluded that not all the soft magnetic α-Fe grains were covered by exchange interactions. In this case, an increase in the cooling rate by increasing the linear speed of the rotating copper drum to 22 m/s should result in hardening of the magnetic properties, because a $Nd_8Tb_2Fe_{81}Zr_1B_6$ alloy with smaller grain sizes would be obtained and phases with different magnetic hardnesses would interact with each other by exchange coupling.

The hysteresis loops for the samples solidified at higher cooling speeds were of a wasp shape, typically encountered in materials containing small inclusions of hard magnetic phase distributed in the amorphous matrix. The exception was the hysteresis loop obtained for the $Nd_{10}Fe_{81}Zr_1B_6$ alloy that was solidified at the fastest cooling rate. It had a typical shape characteristic for a magnetically soft material. In this case, the low content of crystalline phase only slightly affected the shape of the hysteresis loop, mainly by increasing the coercivity field (relative to a fully amorphous alloy).

4 CONCLUSIONS

On the basis of X-ray studies, it was found that the samples made with the 20 m/s linear velocity of the copper cylinder were crystalline and consisted of two phases: α-Fe and $RE_2Fe_{14}B$. A qualitative analysis of the phase composition showed that the contents of both phases were 19.15 and 19.40 of α-Fe phase, 80.85 and 80.60 of $Nd_2Fe_{14}B$ phase, for $Nd_{10}Fe_{81}Zr_1B_6$ and $Nd_8Tb_2Fe_{81}Zr_1B_6$ alloys, respectively. The grain size analysis based on Bragg's equation showed that the grains in the alloy containing Tb were almost two times larger. Alloys obtained with higher linear speeds of the copper drum (30 m/s and 35 m/s) were mainly amorphous and contained only small amounts of crystalline phase precipitates.

From the magnetic studies it was found that the tapes produced with the lowest cooling rate were characterized by the best hard magnetic properties. The application of higher speeds of the copper drum resulted in their deterioration.

The hysteresis loop of $Nd_{10}Fe_{81}Zr_1B_6$ (obtained at 20 m/s) was smooth due to presence of strong exchange coupling between the phases of different magnetic hardness. The substitution of Nd by Tb in these samples resulted in an improvement of the saturation magnetization and in a significant increase in the coercivity, but also resulted in the formation of a bimodal shape for the hysteresis loop. The reason for this was decoupling of

the exchange interaction due to an increase of the grain sizes of both phases. Summarizing, for alloy with Tb addition, an increase in the linear speed of the rotating copper drum from 20 m/s to 22 m/s should result in a hardening of the magnetic properties.

5 REFERENCES

[1] Y. Sen, S. Xiaoping, D. Youwei, Exchange coupled $Nd_2Fe_{14}B/\alpha$-Fe nanocomposite magnets with fine α-Fe grains, Microelectron. Eng., 66 (**2003**), 121–127, doi:10.1016/S0167-9317(03)00035-2

[2] R. Fischer, T. Schrefl, H. Kronmuller, J. Fidler, Phase distribution and computed magnetic properties of high-remanent composite magnets, J. Magn. Magn. Mater., 150 (**1995**), 329–344, doi:10.1016/0304-8853(95)00298-7

[3] E. F. Kneller, R. Hawig, The Exchange-Spring Magnet: A new material principle for permanent magnets, IEEE Trans. Magn., 27 (**1991**) 4, 3588

[4] C. Wang, M. Yan, Q. Li, Effects of Nd and B contents on the thermal stability of nanocomposite $(Nd,Zr)_2Fe_{14}B/\alpha$-Fe magnets, Mater. Sci. Eng. B, 150 (**2008**) 77, doi:10.1016/j.mseb.2008.02.007

[5] B. Xiaoqian, Z. Jie, L. Wei, G. Xuexu, Z. Shouzeng, Influence of zirconium addition on microstructure, magnetic properties and thermal stability of nanocrystalline $Nd_{12.3}Fe_{81.7}B_{6.0}$ alloy, Journal of Rare Earths, 27 (**2009**), 843, doi:10.1016/S1002-0721(08)60347-6

[6] Z. Tian, S. Li, K. Peng, B. Gu, J. Zhang, M. Lu, Y. Du, The microstructure and magnetic properties of NdFeB magnets directly solidified at a low cooling rate, Mater. Sci. Eng. A, 380 (**2004**), 143, doi:10.1016/j.msea.2004.03.077

[7] A. Ceglarek, D. Płusa, P. Pawlik, M. Dośpiał, Influence of heat treatment on magnetic properties of nanocrystalline $Nd_9Fe_{84}Zr_1B_6$ ribbons received by rapid solidification method, Arch. Metall. Mater., 57 (**2012**), 229–232, doi:10.2478/v10172-012-0015-6

[8] H. Sheng, X. Zeng, D. Fu, F. Deng, Differences in microstructure and magnetic properties between directly-quenched and optimally-annealed Nd–Fe–B nanocomposite materials, Physica B, 405 (**2010**), 690, doi:10.1016/j.physb.2009.09.088

[9] A. E. Ceglarek, D. Plusa, M. J. Dospial, M. G. Nabialek, P. Pietrusiewicz, Investigation of the Magnetization Reversal Process of High-Remanent $Nd_{10}Fe_{83}Zr_1B_6$ Alloy in the As-Cast State, Acta Phys. Polon. A, 121 (**2012**), 1279–1281

[10] J. C. Martínez-García, J. A. García, M. J. Rias, Asymmetric magnetization reversal of partially devitrified $Co_{66}Si_{15}B_{14}Fe_4Ni_1$, Non-Cryst. Solids, 354 (**2008**), 5123–5125, doi:10.1016/j.jnoncrysol.2008.05.059

[11] M. Dośpiał, J. Olszewski, M. Nabiałek, P. Pietrusiewicz, T. Kaczmarzyk, The microstructure and magnetic properties of $Nd_{8.5}Tb_{1.5}Fe_{83}Zr_1B_6$ ribbons obtained at various cooling ratek, Nukleonika, 60 (**2015**) 1, 15–18, doi:10.1515/nuka-2015-0005

[12] M. Dospial, D. Plusa, B. Ślusarek, Study of the magnetic interaction in nanocrystalline Pr–Fe–Co–Nb–B permanent magnets, J. Magn. Magn. Mater., 324 (**2012**), 843–848, doi:10.1016/j.jmmm.2011.09.029

[13] H. Kronmüller, M. Fähnle, Micromagnetism and the microstructure of ferromagnetic solids, Cambridge University Press, Cambridge, United Kingdom 2003

[14] G. K. Williampson, W. H. Hall, X-ray line broadening from filed aluminium and wolfram, Acta Metallurgica, 1 (**1953**) 22, doi:10.1016/0001-6160(53)90006-6

[15] J. D. Livingston, The history of permanent-magnet material, Journal of Metals, 2 (**1990**), 30-34

[16] M. Dospial, D. Plusa, Magnetization reversal processes in bonded magnets made from a mixture of Nd-(Fe,Co)-B and strontium ferrite powders, J. Magn. Magn. Mater., 330 (**2013**), 152–158, doi:10.1016/j.jmmm.2012.10.022

[17] R. W. Gao, D. H. Zhang, W. Li, X. M. Li, J. C. Zhang, Hard magnetic property and $\delta M(H)$ plot for sintered NdFeB magnet, J. Magn. Magn. Mater., 208 (**2000**), 239, doi:10.1016/S0304-8853(99)00562-4